American Society of Mechanical Engineers

ASME Accepted Manuscript Repository

Institutional Repository Cover Sheet

Cranfield Collection of E-Research - CERES

ASME Paper Title: Comparison of tabulated and complex chemistry turbulent-chemistry interaction models with high fidelity large eddy simulations on hydrogen flames

Authors: M. Zghal , X. Sun , P. Q. Gauthier , V. Sethi

ASME Conf Title: **ASME Turbo Expo 2020**

Volume/Issue: _Volume 3_____ Date of Publication (VOR* Online) 11 January 2021 _____

ASME Digital Collection URL: https://asmedigitalcollection.asme.org/GT/proceedings/GT2020/84119/V003T03A014/1094633

DOI: https://doi.org/10.1115/GT2020-16070

*VOR (version of record)

Proceedings of ASME Turbo Expo 2020
Turbomachinery Technical Conference and Exposition
GT2020

September 21-25, Virtual, Online

GT2020-16070

COMPARISON OF TABULATED AND COMPLEX CHEMISTRY TURBULENT-CHEMISTRY INTERACTION MODELS WITH HIGH FIDELITY LARGE EDDY SIMULATIONS ON HYDROGEN FLAMES

M. Zghal[1], X. Sun*[2], P. Q. Gauthier[3], V. Sethi[2]

[1]Université Laval, Quebec, Quebec, Canada
[2]SATM, Cranfield University, Cranfield, Bedfordshire, UK
[3]Siemens Canada Limited, Montreal, Quebec, Canada

ABSTRACT

Hydrogen micromix combustion is a promising concept to reduce the environmental impact of both aero and land-based gas turbines by delivering carbon-free and ultra-low-NOx combustion without the risk of autoignition or flashback. The EU H2020 ENABLEH2 project aims to demonstrate the feasibility of such a switch to hydrogen for civil aviation, within which the micromix combustion, as a key enabling technology, will be matured to TRL3. The micromix combustor comprises thousands of small diffusion flames where air and fuel are mixed in a crossflow pattern. This technology is based on the idea of minimizing the scale of mixing to maximize mixing intensity. The high-reactivity and wide flammability limits of hydrogen in a micromix combustor can produce short and low-temperature small diffusion flames in lean overall equivalence ratios.

In order to mature the hydrogen micromix combustion technology, high quality numerical simulations of the resulting short, thin and highly dynamic hydrogen flames, as well as predictions of combustion species, are essential. In fact, one of the biggest challenges for current CFD has been to accurately model this combustion phenomenon. The Flamelet Generated Manifold (FGM) model is a combustion model that has been used in the past decades for its predicting capabilities and its low computational cost due to its reliance on pre-tabulated combustion chemistry, instead of directly integrating detailed chemistry mechanisms. However, this trade for a lower computational cost may have an impact on the solution, especially when considering a fuel such as Hydrogen. Therefore, it is necessary to compare the FGM model to another combustion modelling approach which uses more detailed complex chemistry.

The main focus of this paper then, is to compare the flame characteristics in terms of position, thickness, length, temperature and emissions obtained from LES simulations done with the FGM model, to the results obtained with more complex chemistry models, for hydrogen micromix flames. This will be done using STAR-CCM+ to determine the most suitable numerical approach required for the design of injection systems for ultra-low NOx.

Keywords: Hydrogen; micromix; Combustion; ENABLEH2; STAR-CCM+; FGM Kinetic rate; Thickened Flame; Complex Chemistry; Eddy Dissipation Concept;

NOMENCLATURE

c	Progress variable
Da	Damköhler number
D_{lam}	Laminar Diffusivity
E	Efficiency factor
F	Thickening factor
f	Mean reaction rate multiplier
Ka	Karlovitz number
l_o	Integral length
r_k	reaction rate
R_{et}	Turbulent Reynolds number
S_L	Laminar flame speed
Sc_t	Turbulent Schmidt number
T	Temperature
u’	Turbulence intensity (speed)
v	Kinematic viscosity
W_i	Species-specific weight
Y_i	ith species’ mass fraction

* Address all correspondence to this author: x.sun@cranfield.ac.uk

Copyright © 2020 by ASME

Published by The American Society of Mechanical Engineers. This is the Author Accepted Manuscript issued with:
Creative Commons Attribution License (CC BY). The final published version is available online at DOI:10.1115/GT2020-16070.
Please refer to any applicable publisher terms of use.

y	unnormalized progress variable
Z	Mixture fraction
δ_L	Laminar flame thickness
η	Kolmogorov microscale
Υ	Heat loss ratio
μ_t	Turbulent viscosity
$\dot{\omega}_i$	Net reaction rate of species i
Ω	Reaction zone sensor
φ	Equivalence ratio
ρ	Density
τ	time scale
Ξ	Wrinkling factor

INTRODUCTION

The pollutants emitted by conventional hydrocarbon fuels used in gas turbine applications include carbon dioxide (CO_2), oxides of nitrogen (NOx), carbon monoxide (CO), unburned hydrocarbons (UHC) and soot. These pollutants are toxic for humans and contribute to atmospheric pollution and global warming [1]. To protect the environment and achieve a climate neutral economy, the European commission adopted a 2050 long-term strategy that aims to reduce emissions of pollutants by 80 to 95% [2]. To do so, the new technologies developed need to be more sustainable than ever. This implies a switch from fossil fuels to more renewable forms, such as hydrogen. Although hydrogen combustion emits oxides of nitrogen, it mainly produces water and doesn't produce any other pollutants associated with hydrocarbons. Therefore, hydrogen is the ideal fuel to use when aiming to reduce the emissions of pollutants to protect the environment and the human health.

For the gas turbine industry to switch to hydrogen fuels, it is important to develop tools that accurately predict its combustion process. The ENABLEH2 project aims to prove that a switch to liquid hydrogen in the civil aviation field is feasible. One of the key studies of this project is related to maturing hydrogen micromix combustion technology through a combination of numerical and experimental research. A key part of this study will be an analysis of the position, length and temperature of small hydrogen diffusion flames and how these are influenced by micromix injector geometry and spacing. The predictive capability of the hydrogen combustion models currently used in state-of-the-art Computational Fluid Dynamics (CFD) tools namely STAR-CCM+, ANSYS-Fluent and AVBP will also be assessed. This is essential to the development of micromix combustion technology, considering that hydrogen atoms behave differently than traditional fuels. These models will subsequently be validated and calibrated for hydrogen combustion using the data generated from the experiments and will be used for a comprehensive evaluation of the design space for conditions that lie outside the capabilities of the experimental facilities.

One of the biggest challenges for CFD so far has been to accurately model and predict combustion process. The complexity of combustion CFD comes from the simultaneous modeling of the flow's physics and chemical reactions which makes it difficult to predict accurately the emissions of pollutants. For propulsion systems, it is important to predict accurately the flame's length, shape, position and temperature. To do so, the combustion models used in CFD should ideally include and solve a detailed chemistry mechanism. However, the computational cost of modeling complex chemistry limits the accuracy of the combustion models being developed. To reduce the computational cost of combustion modelling, many CFD models are developed for a precise flame's regime. The Borghi diagram has traditionally been a popular tool to characterize the flame's regime, but most found in the literature assume a Lewis number near unity. While this is an acceptable assumption for hydrocarbons, this is not valid for hydrogen because its mass transport is faster than its heat transport which results in a Lewis number less than unity [3]. The modified flame diagram for non-premixed hydrogen flames proposed by M. Lopez [4] was used to characterize the hydrogen flame's regime of this study, which are diffusion flames at an equivalence ratio of 0.5 under a pressure of 15 bar. From this diagram, it was determined that a flamelet combustion CFD model could be used.

The Flamelet Generated Manifold (FGM) model is a promising combustion model with a low computational cost that has been used in the past decades for its predicting capabilities, especially for hydrocarbons combustion [5]. This combustion model assumes that the turbulent flames can be represented by a set of flamelets and parametrize their thermodynamic and chemical states inside a table that is used to model three-dimensional flames. This table contains a minimum number of scalars, hence the FGM model's lower computational cost. However, in order to be a valid approach, this trade for a lower computational cost should not have a major impact on the solution when modelling hydrogen diffusion flames. Therefore, it is necessary to compare the FGM model to another combustion model that uses a more detailed chemistry, such as the Complex Chemistry (CC) model. Unlike the FGM model, the CC model is also suitable for turbulent flow where there is a strong separation between mixing and chemical timescales. To model the turbulence-chemistry interaction with the CC model, the Eddy Dissipation Concept (EDC) model can be used.

Combustion models' sensitivity to the mesh is another factor that increases the computational cost of combustion CFD. For high fidelity approaches such as Large Eddy Simulations (LES), a finer mesh is needed to accurately predict the flame's position, thickness and length. The Thickened Flame Model (TFM) available within STAR-CCM+ addresses the computational cost of mesh refinements by thickening the flame's fronts, which allows to resolve the flame on a coarser volume mesh. This model is only available for LES simulations. The scaling strategy used by the TFM model also raises questions regarding the accuracy of the solution and its applicability to non-premixed flames.

There are a lot of gaps in knowledge when it comes to hydrogen combustion. Most CFD-related numerical studies in the public domain have been limited to hydrogen blends with

Copyright © 2020 by ASME

hydrocarbons rather than pure hydrogen [5, 6, 7]. Regarding pure hydrogen micromix combustion, although the FGM model has been calibrated for this application, this has only been done at low pressure [8]. As for the combustion CFD models, the literature shows that the FGM model and the TFM model have been mainly studied using hydrocarbons and partially premixed flames [9, 10]. For the CC model, the research done mainly studies the chemistry of hydrocarbons and uses acceleration methods to reduce computational cost [11, 12]. To the authors' knowledge, there are no research available in the public domain for the CC model with the TFM model for hydrogen at high pressure and no work comparing the EDC model to the FGM model for hydrogen combustion.

Therefore, the focus of this study is to compare LES and Reynolds-Averaged Navier Stokes (RANS) predictions made by the FGM model to the ones made by the CC model for hydrogen diffusion flames using STAR-CCM+. Hydrogen properties and reaction rates are believed to be drastically influenced by temperature and pressure. Therefore, the predictions of both combustion models are compared under high temperature and high-pressure inlet conditions. Thus, the response of both combustion models to extreme combustion conditions (high pressure and high temperature) is evaluated. This study also addresses the effects of the TFM model on the predictions made by the CC model. In the future, the simulation results generated from this study will be used to evaluate the predictive capability of both models using the data generated from the experimental campaign. This data will subsequently be used to validate and calibrate the combustion models. A key outcome of this will be an assessment of the suitability and limitations of using the lower fidelity models which require lower computational resources for preliminary design space exploration of low-emissions hydrogen micromix combustion systems.

1 HYDROGEN FLAME REGIME

For turbulent premixed combustion, there are three flames regimes; the flamelet regime, the thin reaction zones regime and the broken flame regime [13]. A laminar flame is referred to as a flamelet [13]. Under certain conditions, a turbulent flame can be represented by a set of flamelets [14]. The regime depends on the mixing and chemical characteristics of the flame and can be characterized by the Karlovitz number Ka and the Damköhler number Da. The latter represents the ratio of mixing time to chemical time and is given by equation (1). [13]

$$Da = \frac{\tau_{turb}}{\tau_{ch}} = \left(\frac{S_L}{\delta_L}\right)\left(\frac{l_0}{u'}\right) \quad (1)$$

Where τ_{ch} is the chemical time scale, which is a function of the laminar flame speed S_L and the laminar flame thickness δ_L, and τ_{turb} is the turbulence time scale, which is a function of the integral length l_o scale and the turbulence intensity u'. A high Damköhler number (Da > 1) means that the chemistry happens faster than the mixing. The Karlovitz number represents the ratio of chemical time to turbulence dissipation time. The following equation (2) presents the Karlovitz number as a function of the turbulent Reynolds number and the Damköhler number. [13]

$$Ka = \frac{\tau_{ch}}{\tau_\eta} = \left(\frac{\delta_L}{S_L}\right)\left(\frac{v}{\eta^2}\right) = \frac{\sqrt{Re_t}}{Da} \quad (2)$$

Where τ_η is the Kolmogorov time scale, which is a function of the molecular kinematic viscosity v and the Kolmogorov microscale η. The latter is the smallest turbulence length scale and represents the turbulent kinetic energy dissipation to fluid internal energy [15]. A low Karlovitz number means that the turbulence dissipates at a slower rate than the chemical reactions' rate. The turbulent Reynolds number Re_t presented in equation (3) relates the Kolmogorov length scale to the integral length scale. [13]

$$Re_t = \frac{u' l_0}{v} = \left(\frac{l_0}{\eta}\right)^{4/3} \quad (3)$$

For a high Damköhler number with a small Karlovitz number (Ka < 1) the flame front is not penetrated by the turbulent eddies and the transport of heat and mass inside the flame is mainly controlled by the chemical processes. Therefore, the turbulent flames are considered flamelets. With a relatively high Karlovitz number (1< Ka < 100), turbulence influences the transport properties in the flame, but they are still mainly governed by the chemical processes. This leads to the thin reaction zones regime. For higher Karlovitz numbers and lower Damköhler numbers, the structure of the flame can't be associated with the flamelet's structure and the flame is in the broken flame regime where quenching might occur [13].

Because of the high maximum flame speed associated with hydrogen, the Damköhler number for hydrogen combustion is expected to be high. The laminar flame speed S_L varies proportionally with thermal diffusion. Being a lightweight atom, Hydrogen diffuse faster than any other conventional fuel atoms, hence its higher thermal and mass diffusivity. [15]

Lopez [4] previously studied the flame characteristics and emissions of hydrogen micromix combustor injectors. The geometric model and boundary conditions used in his study are also used in the present study. In the preliminary research of his study and with preliminary LES simulations, he has shown that for hydrogen combustion, the flames studied are expected to be in the thin reaction zones regime with a high Damköhler number. Damköhler numbers Da, Karlovitz numbers Ka, and turbulent Reynolds numbers Re_t were calculated at different operating pressure P ϵ[1,5,10,20] bar and for different equivalence ratio φ ϵ[0.5,2]. The modified Borghi diagram for non-premixed flames presented in Figure 1 contains these values evaluated for an air stream temperature T_{air} of 600K and a hydrogen temperature T_{H2} of 300K.

In Figure 1, the smallest Damköhler number for all pressure evaluated is associated to an equivalence ratio of 0.5 and the flames are predicted to be in the lower limit of the thin reaction zones regime. An increase in pressure could lead to the broken

Copyright © 2020 by ASME

flames' regime due to the resulting higher turbulent Reynolds number. Because the operating pressure of 15 bar is inside the pressure range plotted in Figure 1, the flames of this study are expected to be in the thin reaction zones regime. Therefore, it's possible to model them with the FGM model, which is suitable for flames in the thin reaction zones regime with a high Damköhler number [16].

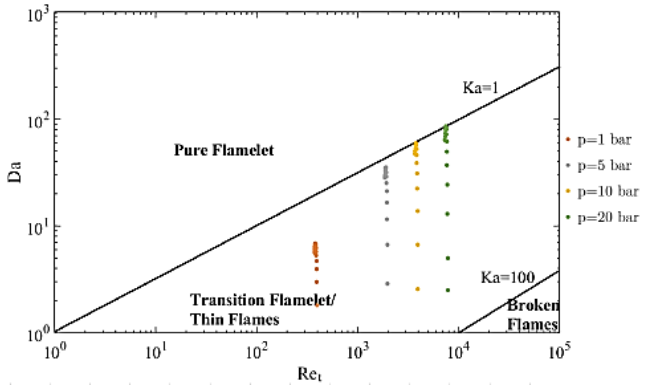

Figure 1: Non-premixed flame diagram for a range of operating pressure P ϵ[1,5,10,20] bar and for different equivalence ratio φ ϵ[0.5,2], at T_{air}=600K and T_{H2}=300K. [4]

2 FLAMELET GENERATED MANIFOLD MODEL

Flamelet models are used for combustion processes where turbulence is not expected to significantly alter the flame structure from that of a laminar flame. The FGM model provides a chemical source term which incorporate finite-rate chemical influence on the flame stabilization. The flamelets are parametrized by mixture fraction Z, heat loss ratio Υ and the progress variable c. The fluctuations due to turbulence in the mixture fraction are accounted for by its variance Z_{var}. The progress variable c indicates the chemical state of the combustion zone and is a normalized value that is calculated using equation (4) [16].

$$c = \frac{y - y_u}{y_b - y_u} \tag{4}$$

Where y, y_b and y_u are unnormalized progress variables. The unnormalized progress variable y is the one of the mixture, y_u is the one at the initial unburnt state and y_b is the one at the burnt state. The unnormalized progress variable of the mixture *y* is defined by equation (5). [16]

$$y = \sum (W_i Y_i) \tag{5}$$

Where Y_i is the ith species' mass fraction and W_i is a species-specific weight used to determine its importance when defining the progress variable. The unnormalized progress variable variance y_{var} is calculated with an algebraic relationship which is defined by the multiplication of a model constant c_v by the product of the square of its gradient and the square of the mesh size Δ. The transport equation of the unnormalized progress variable *y* is given in equation (6). [16]

$$\dot{\omega}_y = \frac{\partial \rho y}{\partial t} + \nabla \cdot (\rho u y) - \nabla \cdot (\Gamma_y \nabla y) \tag{6}$$

Where $\dot{\omega}_y$ is the source term, ρ is the density and Γ_y is the diffusivity which varies with the material properties and is calculated using equation (7).[16]

$$\Gamma_y = \rho D_{lam} + \frac{\mu_t}{Sc_t} \tag{7}$$

Where D_{lam} is the laminar diffusivity, μ_t is the turbulent viscosity and Sc_t is the turbulent Schmidt number. The term on the far-right accounts for turbulent diffusivity. The source term used in equation (6) depends on the progress variable source selected. Unlike the others progress variable sources available, the FGM Kinetic Rate model doesn't assume where the reaction occurs in the system to position the flame [16]. The governing equations used during the tabulation process depends on the reactor type selected. For diffusion flames, a 0D Constant Pressure reactor type generates the FGM tables. The governing equations for the tabulation process using the 0D Ignition reactor type are given in equation (8). [16]

$$\frac{\partial T}{\partial t} = -\sum_{i=1}^{N} \frac{h_i \left(\frac{\partial Y_i}{\partial t}\right)}{C_p} \tag{8}$$

Where C_p is the heat capacity and h_i the enthalpy of the i^{th} species. The governing equations presented in equation (8) are solved for each mixture fraction Z and each heat loss ratio Υ. During the integration of the FGM tables, the turbulent fluctuations are accounted for by Probability Density Functions (PDF). For the mixture fraction Z and the progress variable c, the fluctuations are accounted for by a Beta PDF. For the heat loss ratio Υ, a delta function is used. A beta PDF $P_c(c|Z)$ is parametrized by the normalized progress variable c and its variance while being conditioned on mixture fraction to account for the turbulent fluctuations of the progress variable c. A beta PDF $P_Z(Z)$ is parametrized by the mixture fraction Z and its variance Z_{var} to model the turbulent fluctuations of the mixture fraction Z. The density weighted averages of the mixture fraction and its variance, the progress variable and its variance and the heat loss are obtained after the integration of the FGM table. For each parameter, the average quantity Q is integrated by using equation (9). [16]

$$\tilde{Q}(\tilde{Z}, \tilde{c}, \tilde{\gamma}, \tilde{Z}_{var}, \tilde{c}_{var}) = \int_0^1 \int_0^1 Q(Z, c, \tilde{\gamma}) P_c(c|Z) P_Z(Z) dZ dc \tag{9}$$

During the simulation, the FGM model interpolates these variables from the table generated to model the turbulent flames. [16]

3 COMPLEX CHEMISTRY MODEL

Unlike the FGM model, the Complex Chemistry model can model the turbulence-chemistry interactions and doesn't assumes that turbulent flames can be represented by flamelets. It is suitable to model turbulent flames where the turbulent mixing happens faster than the reactions. The computational

Copyright © 2020 by ASME

cost of the CC model is higher than the FGM model because it uses a more detailed chemistry to model the combustion process. [16]

The CC model uses a species transport equation to solve the chemistry. The integration of the chemical source terms is done by the CVODE solver assuming a constant pressure reactor. The species transport equation is given in equation (10). [16]

$$\omega_i = \frac{\partial}{\partial t}\rho Y_i + \frac{\partial}{\partial x_j}(\rho u_j Y_i + F_{k,j}) \quad (10)$$

Where ω_i is the source term, which is the net rate of production of the species I, and $F_{k,j}$ is the diffusion flux which is calculated using Fick's law. The species transport equation presented in equation (10) is solved using an operator splitting algorithm that integrates the chemical state before solving the transport equation with an explicit reaction source term. The chemical state of each cell is integrated every time step τ_{int} using equation (11). [16]

$$Y_i^* = Y_i + \int_0^{\tau_{int}} r_k(\mathbb{Y}, T, p)dt \quad (11)$$

Where Y_i* is the mass fraction of the chemical state after the time step, r_k is the reaction rate, T is the temperature and $\mathbb{Y}$ is the species mass fraction vector. The source term for the i^{th} species ω_i is then solved using equation (12). [16]

$$\omega_i = \rho f\left(\frac{Y_i^* - Y_i}{\tau_{int}}\right) \quad (12)$$

Where *f* is the mean reaction rate multiplier. The latter and the integration time τ_{int} depends on how the turbulence-chemistry interaction is modeled. The Eddy Dissipation Concept (EDC) is a turbulence-chemistry interactions model that is suitable for diffusion flames and that considers the effects of turbulence when solving the species transport equation by applying a mean reaction rate multiplier *f* lower than 1 that is calculated using equation (13) [16].

$$f = \left(\left[C_l\left(\frac{v\tau_{turb}}{L^2}\right)^{0.25}\right]^{-3} - 1\right)^{-1} \quad (13)$$

Where τ_{turb} is the turbulent time scale, L is the turbulent length scale and C_l is the fine structure length factor which has a default value of 2.1377. The turbulent time scale τ_{turb} is given by the Kolmogorov turbulent time scale τ_η multiplied by a constant that has a default value of 0.4082. During unsteady simulations with the EDC model, the time-step τ over which the chemical state of each cell is integrated is given by the turbulent time scale τ_{turb} multiplied by a scaling factor which has a default value of 1. For a steady state model, the time-step τ_{int} is calculated with the approximate residence time in the cell τ_{res} instead of the turbulent time scale τ_{turb}. [16]

The governing equations of the CC model are also solved with the CVODE solver and are presented in equation (14). [16]

$$\frac{\partial T}{\partial t} = -\sum_{k=1}^{N}\frac{h_i\dot{\omega}_i}{C_p\rho} = -\sum_{k=1}^{N}\frac{h_i}{C_p}\left(\frac{\partial Y_i}{\partial t}\right) \quad (14)$$

Where $\dot{\omega}_i$ is the net reaction rate of species i and h_i is the enthalpy of species i. The ordinary differential equation presented in equation (11) is then integrated using Jacobian matrices to calculate the chemical state within a cell, which makes the CC model computationally expensive. Although there are different acceleration methods available, none are used in the current study. [16]

4 THICKENED FLAME MODEL

Since the flame thickness is usually thin, especially for premixed laminar flames, the mesh resolution required to resolve the flame's internal structure is high. Because the flame speed is determined by the flame's internal structure, a fine mesh resolution is essential to ensure its accurate prediction. The high maximum flame speed associated with hydrogen combustion results in thinner flames, due to the flame thickness being inversely proportional to the flame speed [15]. Therefore, the mesh resolution required is also high for hydrogen diffusion flames.

The Thickened Flame Model (TFM) resolves the flame fronts without the expensive computational cost associated with a fine mesh resolution by artificially thickening them to resolve them directly on the mesh. To do so, the thermal and species local diffusivities are increased while the laminar flame speed is kept unchanged by adjusting kinetic constants. [16]

The TFM model thickens the flame by using a thickening factor F that multiplies local diffusivities and divides the reaction rate. Since the Damköhler number Da is inversely proportional to the flame thickness, increasing the flame thickness by a factor F will also decreases the Damköhler number by the same factor which reduces the flame's sensitivity to the turbulent mixing done by vortexes smaller than the mesh size Δ multiplied by F. An efficiency factor E is introduced to correct the sub grid scale effect of the thickening factor F on the flame front wrinkling. After the thickening of the flame, the efficiency factor E multiplies the diffusivities and the reaction rate to account for the vortexes smaller than the thickened flame. [16]

The artificial thickening provided by the TFM model happens only in the region of the flame fronts to ensure that the flow field characteristics aren't affected by the increased diffusivities. The thickened zone is controlled by the reaction zone sensor Ω. The thickening factor F is a function of the reaction zone sensor Ω and is calculated with equation (15). [16]

$$F = 1 + (F_{max}^{loc} - 1)\Omega \quad (15)$$

Where F_{max}^{loc} is the maximal thickening factor that can be applied within a cell, which is depends on the flame's number of cells and the maximum flame thickening factor. The methods to calculate the flame reaction zone sensor Ω depends on the combustion model selected. For the CC model, the turbulence-chemistry interaction is defined by the TFM model instead of the EDC model. The reaction zone sensor can be calculated with the reaction rate method by using equation (16). [16]

$$\Omega = tanh\left(\beta_\Omega\frac{\omega}{\omega_{max}}\right) \quad (16)$$

Where β_Ω is a constant with a default value of 100 that controls the gradients nearby the flame fronts' edges, ω is the cell

Copyright © 2020 by ASME

reaction rate and ω_{max} is the maximum reaction rate in the domain. Unlike the other models available to calculate the efficiency factor E, the Wrinkling Factor Ratio model is based on DNS data and spectral analysis done by Colin & al. [20]. With the Wrinkling Factor Ratio model, the efficiency factor E is the ratio of the wrinkling factor of the laminar flame to the wrinkling factor of the thickened flame. The expression of the wrinkling factor is given by equation (17). [16]

$$\Xi = 1 + \frac{u'_{\Delta e}}{S_L}\left(\frac{2\ln 2}{3c_{ms}(\sqrt{Re_t}-1)}\right)\left(0.75e^{\left[-1.2\left(\frac{u'_{\Delta e}}{S_L}\right)^{-0.3}\right]\left(\frac{\Delta_e}{\delta_L}\right)^{2/3}}\right) \quad (17)$$

Where $u'_{\Delta e}$ is the turbulent velocity in the local subgrid scale, Δ_e is the local filter size and c_{ms} is a constant. With the Power Law Thermal Diffusivity, the laminar flame thickness is calculated with equation (18). [16]

$$\delta_L = 2\frac{\alpha_u}{S_L}\left(\frac{T_b}{T_u}\right)^{0.7} \quad (18)$$

Where T_b is the burnt temperature, T_u is the unburnt temperature and α_u the unburnt thermal diffusivity. With STAR-CCM+, the correlations available to calculate the laminar flame speed S_L that is used with the TFM model are fuel dependent and were only developed for hydrocarbons [16]. Therefore, they cannot be used with hydrogen and a user-function must be defined to calculate the laminar flame speed. This function is discussed in the methodology section.

5 METHODOLOGY

5.1 Geometry, mesh and boundary conditions

A double injector combustor was used to model the hydrogen diffusion flames of this study. This allows to study the flame characteristics of two single flames. The geometry used is presented in Figure 2.

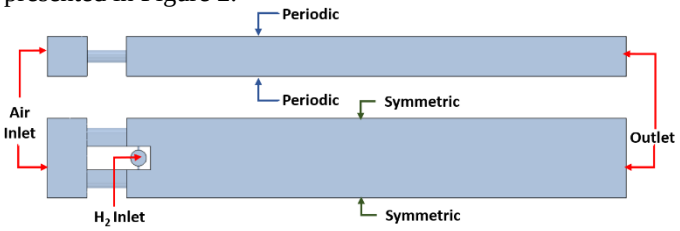

Figure 2: Geometry of the double injector combustor used.

To help the convergence of the simulations using the CC model, a slightly converging 0.5m liner was added at the end of the geometry presented in Figure 2. Both inlets are mass flow inlets with values set so that the equivalence ratio is 0.5. The outlet of the domain is a pressure outlet and the operating pressure is 15 bar. For the temperature, the air at the inlet is at 600K and the hydrogen at the inlet is at 300K. To represent the large number of injectors that will be used for testing, the boundary of the side walls is set to periodic and the boundary of the top and bottom walls is set to symmetric. The same mesh is used by all simulations, even with the TFM model activated. This allows to compare the results independently of the mesh and to validate the prediction capabilities of the TFM model. The mesh is made of polyhedral cells and is fine enough to obtain a courant number near or below unity in the flame region during the LES simulation and to accurately resolve the flame internal structure. The maximum cell size was set to 0.25mm, the base size to 1mm and the volumetric growth rate to 1.1 to ensure a smooth transition. Many surface refinements were added to capture the flow inside the fuel injectors and air channels and to ensure a convective courant number near unity in those problematic regions. The mesh was refined to a cell size of 0.06mm in the region where the air meets with the fuel and in the flame region, which was determined to be 22 mm long by preliminary simulations. The mesh has 8.245 million elements for the RANS simulations and the FGM simulations in LES and has 9.372 million elements for the simulations in LES of the CC model with the EDC model and the CC model used with the TFM model. The increase in elements is due to the addition of a longer liner.

5.2 Physic models

To model the combustion process, a chemistry mechanism is required by both the FGM model and the CC model. An investigation of existing reaction mechanisms for hydrogen combustion, with air, was previously done by G. Babazzi et. al. [17]. This study recommends using the chemistry mechanism proposed by C. V. Naik for hydrogen combustion which considers 9 species (H_2, H, O_2, O, OH, HO_2, H_2O_2, H_2O and N_2) and includes 25 reactions. The NOx emissions are activated in the RANS simulations as a post processing step [18]. Because the Naik mechanism doesn't include the chain reactions for NOx, its emissions are modeled with the NOx thermal model and thus, the NOx Zeldovich mechanism provided by STAR-CCM+. For the CC model, the NOx Zeldovich model uses O and OH concentration.

The species weights W_i used to calculate the unnormalized progress variable *y* is set to 1 for H_2O and to 0 for the other species to indicate that the combustion is completed when the mass fraction of water reaches its maximum value. Although other intermediate species are produced, the main product of hydrogen combustion is water. Therefore, this simplification for the species weight should not have a significant impact on the solution. However, future work should be done to analyze the effect of accounting for other intermediate species if they are important for flame stabilization [16].

Every simulation is three dimensional, adiabatic and uses the ideal gas model with the segregated flow model and the segregated fluid enthalpy model. The RANS steady simulations use SST K-omega turbulence and the flow is incompressible. The LES simulations use the WALE Sub grid Scale model, the implicit unsteady solver is set to second order and the flow is compressible. With the multi-component gas model, the dynamic viscosity is calculated using Sutherland's Law with

Copyright © 2020 by ASME

the default values. The molecular diffusivity is accounted for through a Schmidt number. Lopez [4] previously studied the flame characteristics of hydrogen micromix combustor injectors. For the same geometry and boundary conditions used, but with an equivalence ratio of 0.4, it was found that a Schmidt number of 0.238 models more accurately the fluid properties upstream of the reaction. For the Lewis number, the FGM model assumes a value of 1 [16]. To maintain a similarity between the solving procedure of the FGM model and the CC model, the Lewis number of the latter was also set to 1. Moreover, all the RANS and LES simulations used the same values of turbulent Prandtl and turbulent Schmidt number.

For the TFM model, the values for the maximum flame thickening factor and the number of cells were left constant, since this study is not focused on calibrating the TFM model. For the laminar flame speed, since the available correlations are for hydrocarbon fuels, a user-function must be defined. Ravi et al. [19] developed the correlation presented in equation (19) to calculate the laminar flame speed based on temperatures, pressure and equivalence ratio.

$$S_L = [a_1 + a_2\emptyset + a_3\emptyset^2 + a_4\emptyset^3 + a_5\emptyset^4]\left[\frac{T_u}{T_{ref}}\right]^{(b_1+b_2\emptyset+b_3\emptyset^2+b_4\emptyset^3)} \quad (19)$$

The correlation presented in equation (19) is valid for temperature between 270K and 620K and over the range of pϵ[1,30]atm and φϵ[0.5,5]. The coefficients *a* and *b* for a pressure of 10 atm and 20 atm over the range φϵ[0.5,2] were developed for a reference temperature of 320K, which is close to the initial hydrogen temperature of 300K. The coefficients for the laminar flame speed correlation at 15 atm were interpolated from the coefficient values obtained by Ravi et al at 10 atm and 20 atm. The laminar flame speed correlation error is ± 13cm/s [19]. At ambient temperature and pressure, the flame speed of hydrogen can reach 210 cm/s [15]. Under this condition, the correlation's incertitude represents ± 6.2% of the flame speed. Since the temperature is expected to be higher and because the flame speed increases with the unburned temperature, the correlation's incertitude at ambient pressure is expected to be lower than ± 6.2% of the flame speed. If we consider that the operating pressure is also higher and that the flame speed decreases with pressure, the correlation's incertitude at ambient temperature is expected to increase. Because the flame speed varies less with pressure than with temperature [15], the effect of the latter is considered more significant. Thus, the correlation's incertitude at high pressure and high temperature is expected to be near ± 6.2% of the flame speed. Although this does not account for errors made by the authors while developing the correlation, it is considered an acceptable correlation to use. In the future, more work should be done to develop and implement laminar flame speed correlations for hydrogen within the TFM model.

Regarding the simulation procedure, for each combustion model a RANS simulation initialize the LES simulation without the TFM model. Before starting to monitor time-averaged values, the LES simulations are run at least two times the residence time. For the TFM model, only its effects using the CC model are analyzed. The LES simulation of the CC model with the EDC model that ran before the time-averaging process is used to initialize the LES simulation with the TFM model. To obtain a courant number near or below unity in the flame region, the time-step for every LES simulation is 0.9μs. Furthermore, the number of inner iterations during each time step time is set to 35 to ensure the residuals converge to the second or third order of magnitude. As a result, more than 90% of the turbulent kinetic energy spectrum was resolved during the LES simulations, which was calculated using half of the sum of the variance of the velocity components.

6 RESULTS AND DISCUSSION

To compare the LES and RANS predictions made by the FGM model to the ones made by the CC model with and without the TFM model, the values are normalized over the range of the selected scale In all figures, *LES($\bar{t}$)* represents time-averaged contours and *LES(t_i)* instantaneous contours.

For diffusion flames, combustion takes place where the air and fuel are in stoichiometric proportion. At the flame's surface, the mixture fraction Z is stoichiometric and equals to the stoichiometric mass fraction of fuel [15]. Therefore, it is possible to visualise the flame by locating where in the domain the mass fraction of hydrogen is near its stoichiometric value of 0.0285. The contours of hydrogen's mass fraction near its stoichiometric value are shown in Figure 3.

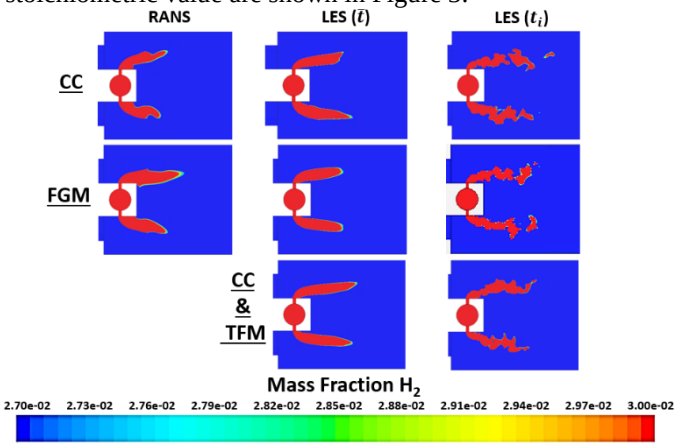

Figure 3: Contours of the mass fraction of H_2.

It is possible to observe in Figure 3 that for the RANS simulations, the FGM model predicts asymmetric flames in terms of length and thickness, and the CC model with the EDC model slightly in terms of shape. The FGM model RANS simulation predicts that the lower flame is thinner and 23.68% shorter than the upper flame. It also predicts thicker flames compared to the CC model with the EDC model. As for the flame's position, the latter predict flames that are more detached from the walls and that are on average 7.39% higher than the FGM model. Furthermore, for the RANS simulation, the FGM model predicts flames that are on average 22.14% longer than the ones predicted by the CC model used with the EDC model.

Copyright © 2020 by ASME

By modeling the turbulence-chemistry interactions, the effect of turbulence on combustion is accounted for through an increased turbulent diffusivity [16]. This results in a higher flame speed propagation and an increased turbulent mixing [16]. Because the combustion process in diffusion flames depends more on the mixing rates than on the chemical rates [13], considering the effect of turbulence leads to a faster consumption rate, which results in a shorter flame. The FGM Kinetic Rate model doesn't consider that the internal structure of the flame is driven by turbulence like the EDC model does for the CC model's species chemical source term by applying a mean reaction rate multiplier f lower than 1 in equation (12), which explains why the flame predicted by the FGM model is longer. This also means that the FGM model predicts a slower flame propagation, which results in a higher residence time, hence a thicker flame. Because the flame propagation speed modifies its position, this also explain why the latter predicts a lower flame height. Furthermore, when the turbulent mixing is faster than the chemical reactions, the shear layer between hydrogen and fuel often stretch and curve and the flame front appears more wrinkled due to turbulence [13]. This explains the wrinkled shaped flame predicted by the RANS simulation of the CC model with the EDC model.

For the time averaged LES simulations, the FGM model predicts thicker symmetric flames while the CC model with the EDC model predicts asymmetric flames in terms of length. The CC model with the EDC model LES simulation predicts that the lower part flame is on average 18.71% longer than the upper part flame. Furthermore, the average flames length predicted is 28.36% longer than the one predicted by the corresponding RANS simulation. This is the opposite for the FGM model, since the average flames length predicted by the LES simulation is 11.27% shorter than the one predicted by the RANS simulation. These variations in symmetry in terms of thickness and length between the RANS and LES simulations of the FGM model and the CC model with the EDC model could indicate that different states are being predicted by both simulations. The model's sensitivity to the mesh and the boundary conditions might trigger changes in aerodynamics. Coupled with heat release, these changes might be leading to bi-stable solutions. In the future, a full injector array should be modeled to analyze better the flames interactions and remove any potential effect due to the periodic or symmetric boundary conditions being imposed.

For both LES and RANS simulation, the FGM model predicts flames that are slightly thicker. Because of the high maximum flame speed associated with hydrogen combustion, the hydrogen flames are expected to be thin. Thus, it is possible that the FGM model tends to overpredict the flame's thickness, especially when used in a RANS simulation. The FGM model's predictions in terms of thickness need to be validated in the future, when experimental data is available. Because this study is focusing on the effect of using a more detailed chemistry combustion model, the effects of the TFM model when activated with the FGM model was not studied. Future work should be done with the FGM model to analyze the impact of modeling more properly the turbulence-chemistry interactions by using the TFM model. This would allow to study the TFM model impacts on how the progress variable is resolved and how this affects the predicted flames characteristics.

For the LES simulation of the CC model with the TFM model activated, modeling the turbulence-chemistry interaction with the TFM model instead of the EDC model results in flames predicted to be 37.59% longer than the ones predicted by the RANS simulation with the EDC model and 7.19% longer than the ones predicted by the LES simulation with the EDC model. Furthermore, the TFM model predicts a thinner flame when compared to the other simulations (RANS and LES) done with the EDC model. The differences between the predicted results of the EDC model and the TFM model could be due to their respective method of calculation of the laminar flame speed. Since there are no valid correlations for the laminar flame speed of hydrogen in STAR-CCM+, the one developed by Ravi et al. [19] was used. Considering its error of ±13 cm/s, it is possible that the laminar flame speed was overestimated during the simulation. Moreover, because the flames studied are under high pressure conditions, they tend to be thinner which could imply that they are not being resolved well enough to accurately predict the flame speed. The lack of experimental data at high pressure and high temperature regarding the laminar flame speed of hydrogen is a limitation of the TFM model. To highlight the differences between the combustion models, the axial evolution of the average mass fraction of hydrogen along the reaction zone is analyzed and shown in Figure 4.

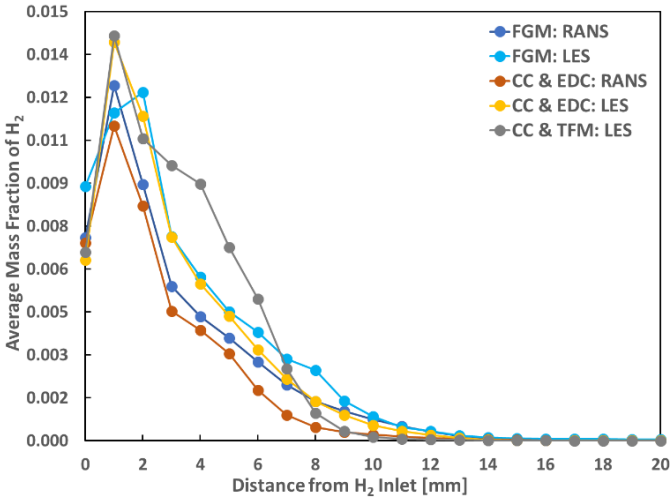

Figure 4: Evolution of the average mass fraction of H_2.

It is possible to observe in Figure 4, that for both LES and RANS simulations, the CC model with the EDC model is predicting a faster consumption of hydrogen than the FGM model. This could be related to the turbulence-chemistry interactions being accounted for in the CC model with EDC model, which results in being able to model a combustion process where the turbulent mixing is very rapid, such as in micromixed flames. On average, it is the CC model used with

Copyright © 2020 by ASME

the TFM model that is predicting the slowest consumption of hydrogen along the reaction zone. This observation relates well to the TFM model prediction of longer flames. Furthermore, the RANS simulations for the CC model with the EDC model and the FGM model are predicting that hydrogen is consumed sooner than their respective LES simulations, thus at a faster rate. During the LES simulations, the wall functions solved differently the flow going through the air channels, which increased their effective area compared to the ones predicted by the RANS simulations, thus predicting a lower air velocity at their outlet. Because the flame's position is influenced by the jet and cross flow characteristics, this caused the hydrogen to penetrate the combustion domain less horizontally and at a slower velocity. This resulted in a slower flame propagation in the domain. Furthermore, the LES simulation capacity to model the small turbulent scales and to resolve the larger ones, which is important considering that diffusion flames are formed due to turbulent mixing in the shear layer between fuel and oxidizer, lead to the prediction of larger vortexes below the jet and cross flow where the reactions are predicted to occur. Thus, the predicted residence time increased and, unlike the RANS simulations, less unconsumed hydrogen is predicted to be diffused inward between both flames near the injectors, which occurs downstream of the injectors, when the flow becomes less influenced by the recirculation zones. The slower flame speed propagation, the higher residence time and the reduced inward diffusion of hydrogen near the injectors predicted by the LES simulations might explain why hydrogen is predicted to be consumed later in the domain.

For the CC model with the EDC model, the additional turbulence modeling provided by the LES simulation seems to capture the local species transport inside of the flame, which locally creates zones poor in hydrogen. This seems to contribute to local quenching and to the extension of the combustion process further downstream of the recirculation zones compared to the corresponding RANS simulation. Combined with the slower flame speed propagation and higher residence time caused by the added turbulence modeling of the LES simulation, the latter predicts longer flames than the corresponding RANS simulation. Moreover, the flames' shape seems to be more influenced by the recirculation zones, which makes the flame front appears less wrinkled.

For the FGM model, the propagation of hydrogen in the domain is not as uniform when the effect of turbulence is added through LES. Just like its corresponding RANS simulation, the FGM model LES simulation predicts a slower flame speed propagation than the one predicted by the CC model with the EDC model because it doesn't model turbulence-chemistry interaction. Combined with the reduced air channels outlet velocity, the FGM model LES simulation predicts that hydrogen penetrates the slowest the reaction zone. Therefore, the velocity in the recirculation zones is lower and the flow is less attached to the them. This allows unconsumed hydrogen to diffuse inward from them more easily than the CC model with the EDC model LES simulation. Because this diffusion still occurs downstream of the injectors, it is more difficult to identify the flames' position. This could explain why the FGM model LES simulation predicts an average flames length that is shorter than its RANS simulation, while simultaneously predicting that hydrogen is completely consumed later in the combustion domain. Furthermore, because the turbulence-chemistry interaction and the turbulent effect on combustion are accounted for by the CC model with the EDC model, the turbulent mixing in the recirculation zones is captured better compared to the FGM model LES simulation. Therefore, the CC model with the EDC model LES simulation predicts there is less unconsumed hydrogen to be diffused inward between both flames from the recirculation zones. This could explain why the latter predicts flames that are longer than the ones predicted by the FGM model LES simulation, while simultaneously predicting that hydrogen is consumed sooner in the combustion domain.

The FGM model assumes that the species molecular and thermal diffusivities are close, which results in a Lewis number near unity. This is not valid for hydrogen because its mass transport is faster than its heat transport, which results in a Lewis number less than one [3]. Therefore, heat accumulates locally during hydrogen combustion which results in the local increase of burned gas temperature. The contours of normalized temperature are shown in Figure 5.

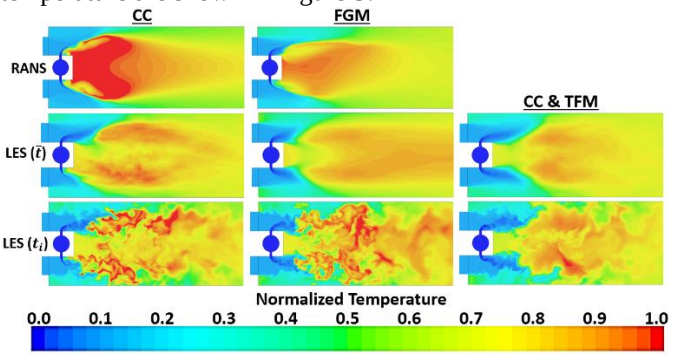

Figure 5: Contours of normalized temperature.

It is possible to observe in Figure 5 that for the RANS and the LES simulations, the FGM model predicts a lower flame temperature near the injector than the CC model with the EDC model. This relates to the faster consumption of hydrogen observed previously for the CC model with the EDC model. Because hydrogen is consumed sooner in the reaction zone, heat will locally be released closer to the fuel inlet. The local increase in temperature predicted by the CC model with the EDC model could be related to the effect of properly accounting for the turbulence-chemistry interactions. Indeed, combustion process for diffusion flames where the turbulent mixing is faster than the chemical reactions often results in increased heat release rates, which also modifies the turbulent flow [13].

However, this is not the case for the FGM model, which assumes that the flames can be represented by a set of flamelets. Coupled with its assumption of a Lewis number of one, the FGM model tends to underestimate the temperature near the

Copyright © 2020 by ASME

injectors, but predicts a higher temperature further away from them. Moreover, for the LES simulations, the temperature locally increases in the recirculation zones due to the higher residence time in them. Because the CC model with the EDC model LES simulation predicts that the reactions mainly occur there, the temperature locally drops between both of them. This is not the case for the FGM model LES simulation because more hydrogen diffuses inward from the recirculation zones, which gives a more uniform temperature profile. Furthermore, all LES simulations predict that less heat is being produced locally near the fuel injectors. The differences with the RANS simulations in terms of heat near the inlet is significant and should be verified once the experimental data is available. This could be due to the LES simulation capacity to better model turbulence, as previously explained. The temperature predicted by each model should influence the predictions of NOx production, since NOx emissions are highly dependent on temperature. The contours of normalized NOx are shown in Figure 6 for the FGM model and the CC model with the EDC model using RANS.

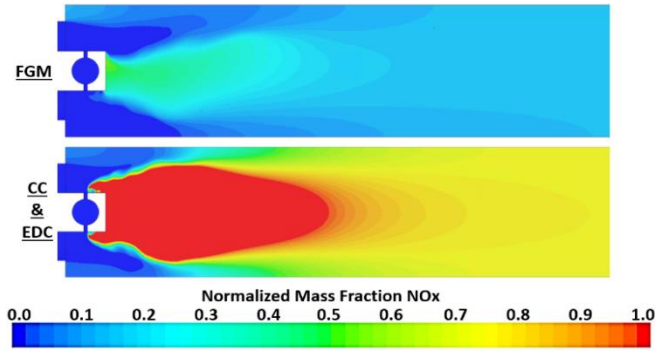

Figure 6: RANS Contours of normalized mass fraction of NOx.

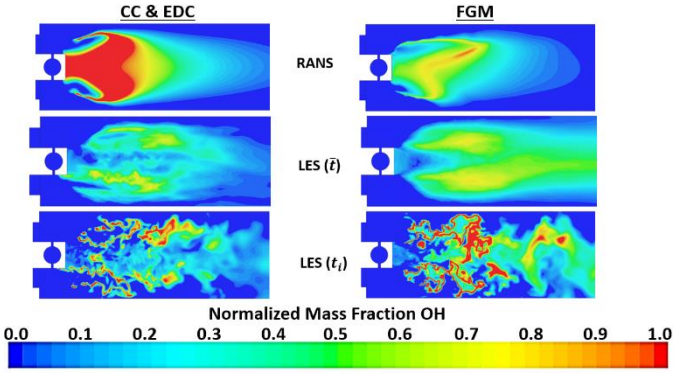

Figure 7: Contours of normalized mass fraction of OH.

It is possible to observe in Figure 6 that for the RANS simulations, the FGM model predicts lower NOx emissions than the CC model with the EDC model. By underestimating the flame's temperature, the FGM model also underestimate significantly the NOx produced. This is caused by the natural increase of NOx emissions with the flame's temperature [1]. It is also interesting to analyze the predictions of the other species involved in the thermal NOx mechanism, such as OH. The contours of normalized OH mass fraction are shown in Figure 7 for the FGM model and the CC model with the EDC model.

It is possible to observe in Figure 7 that for the RANS and the LES simulations, the FGM model predicts lower OH emissions than the CC model with the EDC model. To be produced, NOx requires the presence of OH. Thus, higher OH content can be related to higher NOx emissions. Because the FGM model underestimates OH emissions, the underestimation of NOx was expected. It should be noted that the 0D Ignition reactor type used to generate the FGM tables is known for overpredicting the intermediate species of the reaction, such as OH [16].

However, by not including important minor species such as OH, the progress variable is not able to accurately represent the related chemistry, which could lead to its underprediction when the species is looked up in the flamelet table. This accentuate the relevance of solving the detailed chemistry by accounting for the reaction rates of the mechanism like the CC model does. Due to the computational cost of the latter, future work should be done to overcome the FGM model's underprediction of certain species by modifying the progress variable's definition when generating the flamelet table.

CONCLUSION

This work contributed to obtain a wide variety of results in RANS and LES for the same injector, mesh and boundary conditions, with different combustion models, to analyze the impact of using a combustion model with a more detailed chemistry and the impact of accounting more appropriately for the turbulence-chemistry interactions.

Significant differences in terms of flame's thickness, length, position, temperature and emissions were observed between the predictions made by the Complex Chemistry model used with the Eddy Dissipation Concept model and the Flamelet Generated Manifold model. These differences could be due to the FGM model assuming that the species molecular and thermal diffusivities are close, which is not the case for hydrogen. They could also be explained by the EDC model accounting for the turbulence-chemistry interactions of these hydrogen flames more properly, which leads to their inner structure being driven more by turbulence. Moreover, both combustion models are showing different solutions between their respective LES and RANS simulations, which could be due to the model's sensitivity to the mesh and the boundary conditions triggering changes in aerodynamics that are being coupled with heat release. Regarding the Thickened Flame Model, the flames predicted are significantly thinner and longer than any other combustion model analyzed in this study. This could be due to the laminar flame speed being overestimated due to the high-pressure conditions or due to the laminar flame speed correlation used.

In conclusion, because of the different solutions obtained with LES and RANS for a same combustion model, the predictions need to be validated in the future, when experimental data is available. Moreover, a full injector array should be modeled to analyze if the boundary conditions could be the source of the differences between the solutions obtained. Therefore, the ability of the FGM model to accurately model the combustion

Copyright © 2020 by ASME

of hydrogen within reasonable tolerances has not been invalidated by this study. Moreover, due to the lack of correlations available in the literature for the laminar flame speed of hydrogen at high pressure and temperature, it is not recommended to use the TFM model to model hydrogen combustion at such conditions until further work is done to develop an appropriate correlation with a low incertitude. Afterward, it is highly recommended to calibrate the parameters of the TFM model, such as the maximum thickening factor, for hydrogen combustion. Another important contribution of this study is the use of LES, which blurred the differences between the different combustion model analyzed. Therefore, to obtain least uncertainty when modeling hydrogen micromix combustion, it is recommended that future work be done using LES with a non-unity Lewis number by modeling multi-component diffusion for the CC model with the EDC model and to compare the results with the TFM model activated.

ACKNOWLEDGEMENTS

The ENABLEH2 Project is receiving funding from the European Union's Horizon 2020 research and innovation programme under grant agreement Nº 769241.

REFERENCES

[1] A. H. Lefebvre & D. R. Ballal. Gas turbine combustion: alternative fuels and emissions. CRC Press. United State of America, New-York, 3rd edition, 2010.

[2] European Commission. *A European strategic long-term vision for a prosperous, modern, competitive and climate neutral economy*. Brussels, 2018, Document 52018DC0773.

[3] B. E. Gelfand, M. V. Silnikov, S. P. Medvedev & S.V. Khomik. *Thermo-Gas dynamics of hydrogen combustion and explosion*. Springer, 1st edition, Germany, 2012.

[4] M. Lopez Juarez. *CFD evaluation of flame characteristics and emission of H2 micromix combustor injectors*. Cranfield University. United Kingdom, Cranfield, 2019.

[5] J. A. van Oijen, A. Donini, R. J. M. Bastiaans, J.H.M ten Thije Boonkkamp & L. P. H. de Goey. *State-of-the-art in premixed combustion modeling using flamelet generated manifolds*. Progress in Energy and Combustion Science, Volume 57, 2016, pages 30-47.

[6] J. A. van Oijen, R. J. M. Bastiaans & L. P. H. de Goey. *Modeling preferential diffusion effects in premixed methane-hydrogen-air flames by using flamelet-generated manifolds*. European Conference on Computational Fluid dynamics, Lisbon, Portugal, 2010.

[7] G.M. Kosmadakis, D.C. Rakopoulos, C.D. Rakopoulos. *Methane/hydrogen fueling a spark-ignition engine for studying NO, CO and HC emission with a research CFD code*. Fuel, Volume 185, 2016, pages 903-915.

[8] H.H.W. Funke, N. Beckmann, J. Keinz, S. Abanteriba. *Comparison of numerical combustion models for hydrogen and hydrogen-rich syngas applied for dry-low-Nox-Micromix-Combustion*. Asme: Engineering for Gas Turbine Power, Volume 140, issue 8, Fuel, Volume 1865, 2017, GTP-17-1567.

[9] V.R. Hasti, S. Liu, G. Kumar & J.P. Gore. *Comparison of premixed flamelet generated manifold model and thickened flame model for bluff body stabilized turbulent premixed flame*. American Institute of Aeronautics and Astronautics, United States, 2018.

[10] G. Wang, M. Boileau & D. Veynante. *Implementation of a dynamic thickened flame model for large eddy simulations of turbulent premixed combustion*. Combustion and Flame, volume 158, issue 11, 2011, pages 2199-2213.

[11] S. Kong & R.D. Reitz. *Application of detailed chemistry and CFD for predicting direct injection HCCI engine combustion and emissions*. Proceedings of the Combustion Institute, volume 29, issue 1, 2002, pages 663-669.

[12] L. Zhou & H. Wei. *Chemistry acceleration with tabulated dynamic adaptive chemistry in a realistic engine with a primary reference fuel*. Fuel, volume 171, 2016, pages 186-194.

[13] K. Kuo & R. Acharya. *Fundamentals of turbulent and multiphase combustion*. Wiley, 1st edition, United State of America, New-Jersey, 2012.

[14] W. J.S Ramaekers, B. A Albrecht, J. A Oijen van, L. P. H Goey de & R. L. G. M. Eggels. The application of Flamelet Generated Manifolds in partially-premixed flames. Eindhoven University of Technology. Belgium, Château de Limelette, 2005.

[15] S. R. Turns. *An introduction to combustion: concepts and applications*. McGraw Hill, 3rd edition, United State of America, New-York, 2012.

[16] Siemens. STAR-CCM+ User guide theory. STAR-CCM+.

[17] G. Babazzi, P. Q. Gauthier, P. Agarwal, J. McClure & V. Sethi. NOx Emissions Predictions for a Hydrogen Micromix Combustion System. ASME Turbo Expo 2019: Turbomachinery Technical Conference and Exposition. ASME Digital Collection.

[18] P. Q. Gauthier. *Comparison of temperature fields and emissions predictions using both an FGM combustion model, with detailed chemistry, and a simple eddy dissipation combustion model with simple global chemistry*. Proceedings of ASME turbo Expo 2017 : Turbine Technical Conference and Exposition. United-States, Charlotte, 2017, GT2017-65104.

[19] S. Ravi and E. L. Petersen. Laminar flame speed correlations for pure-hydrogen and high hydrogen content syngas blends with various diluents. International Journal of Hydrogen Energy. Volume 37, Issue 27,2012, pages 19177-19189.

Copyright © 2020 by ASME

https://dspace.org/

Comparison of tabulated and complex chemistry turbulent-chemistry interaction models with high fidelity large eddy simulations on hydrogen flames

Zghal, M.; Sun, Xiaoxiao; Gauthier, Pierre Q.; Sethi, Vishal

2021-01-11
American Society of Mechanical Engineers (ASME)
https://doi.org/10.1115/GT2020-16070
Zghal M, Sun X, Gauthier PQ, Sethi V. (2021) Comparison of tabulated and complex chemistry turbulent-chemistry interaction models with high fidelity large eddy simulations on hydrogen flames. In: ASME TurboExpo 2020, 21-25 September 2020, London, Virtual Event. Paper number GT2020-16070

Downloaded from a DSpace repository. https://dspace.org/